Electrochemical and bioelectrocatalytical properties of novel block-copolymers containing interacting ferrocenyl units

M.P. García Armada [a,*], J. Losada [a], F.J. López-Villanueva [b], H. Frey [b], B. Alonso [c], C.M. Casado [c]

[a] Dpto. de Ingeniería Química Industrial, E.T.S.I.I., U.P.M., José Gutiérrez Abascal no. 2, 28006 Madrid, Spain
[b] Institute of Organic Chemistry, Organic and Macromolecular Chemistry, Duesbergweg 10-14, Johannes Gutenberg-Universität Mainz, D-55099 Mainz, Germany
[c] Dpto. de Química Inorgánica, Facultad de Ciencias, U.A.M., Cantoblanco, 28049 Madrid, Spain

ARTICLE INFO

ABSTRACT

The electrochemical characterization of three different polystyrene-*b*-polybutadiene block-copolymers, functionalized with diferrocenylsilane units, is reported. The PB-blocks have been functionalized with different fractions of electronically communicated, PS_m-PB_{n-p} $(HSiMeFc_2)_p$ units, where $m = 615$, $n = 53$, $p = 39$ (**1**), $m = 375$, $n = 92$, $p = 76$ (**2**) and $m = 455$, $n = 204$, $p = 170$ (**3**). Electrochemical characterization has been carried out both in solution and after electrochemical deposition onto platinum electrodes. The bioelectrocatalytical properties of electrodes modified with the polymers in the nicotinamide dinucleotide (NADH) and glucose oxidase (GOx) oxidations have been investigated as a function of the constitution and structure of the polymers. The analytical properties of electrodes modified with these polymers as sensors of NADH and GOx are described. In addition, an amperometric biosensor for glucose, prepared by electrostatic immobilization of glucose oxidase onto a platinum electrode modified with one of the ferrocenyl block-copolymers as an example, has been developed.

© 2008 Elsevier B.V. All rights reserved.

1. Introduction

Incorporation of organometallic groups into polymeric structures leads to materials with unusual and attractive characteristics. New materials with interesting properties for various fields such as electrochemistry, materials science, organic synthesis and catalysis have been reported [1,2]. The excellent thermal and photochemical stability as well as the unique and valuable redox properties of ferrocenes are well known, and in recent years a large number of research groups have investigated various polymer systems with ferrocenyl-containing structures. Different topologies have been developed, containing the ferrocene moieties as part of the backbone or as side group of a linear chain [3,4]. Research in this direction has also been motivated by advances in the field of dendrimer synthesis and this has led to the development of different examples of ferrocene-functionalized dendrimers [5,6].

Block-copolymers may form supramolecular structures and can also be used to create micropatterned surfaces. In solution they form micellar aggregates that can represent a special environment for electrochemistry. This renders them very interesting in this field of science, and therefore the development of ferrocenyl-con-

taining block-copolymers has become an important issue [7–10]. The corresponding methods developed by Nuyken et al. and Frey et al. are based on the controlled anionic and radical polymerization, respectively, and were successfully applied for the copolymerization of vinylferrocene with styrene or other olefinic monomers [11,12]. Balsara et al. showed that a poly(vinylferrocene)-*b*-poly(isoprene) block-copolymer can be successfully applied as heterogeneous catalyst for Michael additions [13]. Intensive research performed by Manners has led to a wide range of examples concerning block-copolymers with a well-defined ferrocene-containing block [14].

Amperometric enzyme electrodes combine the specificity and selectivity of biological molecules with the direct transduction of reaction rate into current response and represent powerful tools in the field of analysis and biotechnology. Poly(ferrocenyl)-based macromolecules have been demonstrated to possess useful properties for the chemical modification of electrodes and also as electrochemical sensors and electrode mediators in biosensors [15–19].

In biosensoric applications polymers containing ferrocenyl groups are combined with enzymes for use in aqueous media. Generally in enzymes the cofactor is buried within the enzyme structure that forms an insulating layer between an electrode and the redox-cofactor of the enzyme bound to the electrode surface. Using a mediator between electrode and enzyme may represent a possibility to increase the sensibility in biosensors. Particularly ferrocenes have been proven to be very useful in this regard, because

of their favorable formal potential with respect to enzyme redox chemistry. Unfortunately, the oxidized ferricinium species is soluble in aqueous media, which leads to undesired dissolution of the film. In the current work, the hydrophobic nature of polystyrene (PS) as one block in block-copolymers consisting of PS and a poly-butadiene block modified with ferrocene units, can impede solubilization of even very ferrocene-rich polymer films after oxidation.

Flavin-dependent oxidases and nicotinamide adenine dinucleotide (NAD/NADH) dependent dehydrogenases have been investigated for a long time because of their important role in many biochemical reactions.

NAD/NADH dependent dehydrogenases need the freely diffusing cofactor NAD^+ to catalyze oxidation of the substrates. The major problem in practical applications of dehydrogenases is the difficulty in the regeneration of the nicotinamide coenzyme. Electro-oxidation of NADH on solid electrodes usually requires high potentials. A large number of redox mediators such a quinones, phenazines or inorganic molecules can be used to shuttle the electrons from NADH to the electrode in order to reduce the overpotential [20–22]. Another approach is the use of suitable electrodes modified with appropriate mediators [23]. A good method to accelerate the NADH oxidation is the use of the diaphorase reaction coupled with an electron mediator as ferrocene and its derivatives [24].

Mechanistic studies have been made on NADH or model compounds and it has been discussed whether the reaction is a two-electron transfer or involves two single-electron transfers. It has been shown that generally mediators of the two-electron–proton acceptor type in contrast to the one-electron non-proton type present high second-order rate constants with NADH and yield enzymatically active NAD^+ as the reaction product [25]. Flavin-dependent oxidases containing tightly bound FAD in the active center of the enzyme can be electrochemically oxidized by electrodes through mediation by redox mediators. Long-range electron transfer to active sites of these enzymes has been demonstrated, both with enzymes in solution and co-immobilized in two- and three-dimensional surface polymer structures [26]. Several authors have reported that polymers and dendrimers functionalized with ferrocene groups can effectively mediate the electron transfer to glucose oxidase [27–29].

Since $FAD/FADH_2$ is a two-electron redox couple and the ferrocene/ferricinium a one-electron couple two one-reduction steps are involved in the electrochemical reoxidation of the reduced enzyme redox center ($FADH_2$).

In the last years we have reported on the synthesis, redox behaviour and electrocatalytic properties of ferrocene-based materials containing dendritic building blocks with interacting ferrocenyl moieties grafted to multifunctional poly(methyl) siloxane backbones. As can be seen in these articles the electrocatalytic activity of these polynuclear organometallic compounds is favoured by the electronic communication and the short distance between adjacent ferrocenyl moieties within the polymer film [16,17]. The suitable distance between metallic centers allows simultaneous or quasi-simultaneous charge transfers to the enzymatic redox sites, decreasing the high overpotentials required for the electrochemical oxidation of the enzymes.

In this study we report an electrochemical study of anionically prepared diblock-copolymers and the use of platinum electrodes modified with them for the electrocatalytic oxidation of NADH and glucose oxidase. The copolymers consist of a 1,2-polybutadiene block (PB) with di(ferrocenyl)silane side groups as electroactive part and a polystyrene (PS) block that is intended to impart additional polymer properties, such as good solubility, film-forming properties and film-stability over multiple redox cycles. The degree of polymerization of both blocks, the polystyrene block as well as the ferrocene-bearing PB-block has been varied by anionic

polymerization and varying fractions of diferrocenylsilanes have been attached.

2. Experimental

2.1. Chemicals and materials

Karstedt's catalyst in xylene (2.1–2.4% Pt) was purchased from ABCR GmbH & Co. KG and used as received. PS_x-b-PB_y with a 100% 1,2-PB content was prepared in 20 g amounts via a simplified anionic polymerization procedure [30], using a specially constructed reactor system suitable for working under high vacuum and pressure. Methanol, dichloromethane and other solvents and reagents were purchased from Acros and used as received or dried as described in the literature. *tert*-Butyllithium was purchased from Acros (1.5 M solution in pentane). B-Nicotinamide adenine dinucleotide (NADH), reduced dipotassium salt, glucose oxidase (GOx) from *Aspergillus niger* (type VII, 221 000 U/g), and glucose were supplied from Sigma. Glucose solutions were allowed to reach mutarotational equilibrium at room temperature for 24 h before use. All other chemicals were analytical grade and were used without further purification. Ultrapure water was used for preparation of the buffers, standards and electrochemistry work.

2.2. Diferrocenylmethylsilane

Ferrocenyllithium was generated in situ via the reaction of ferrocene (4.4 g, 24 mmol) with 20 mmol of *t*-BuLi in a mixture of 15 mL dried THF and 15 mL dried pentane at 0 °C, under an inert atmosphere. After stirring the mixture at this temperature for 30 min, the temperature was lowered to −30 °C and 1.66 g (14.4 mmol) of dichloromethylsilane was added dropwise. After complete addition the reactants were stirred for 30 min at −30 °C. The mixture was allowed to slowly warm to room temperature. Solvents were removed under vacuum, the crude product was dissolved in pentane and LiCl was removed by filtration. Solvent removal yielded an orange solid which was purified by flash chromatography over silica gel using a mixture of petrol ether and dichloromethane (10:1). After purification the product was obtained as dark orange crystals in 39% yield [31].

2.2.1. Functionalization of PS_x-b-PB_y

All catalytic reactions were conducted in parallel using Radley's 12-placed reaction carousel under inert gas (N_2). Two hundred milligrams of block-copolymer and an equimolar amount of diferrocenylmethylsilane according to the double bonds were dissolved in 5 mL of dried toluene and heated to 100 °C. Fifty microlitres Karstedt's catalyst was added and the mixture was stirred at 100 °C for 3 days. The polymer was purified by repeated precipitation from THF/methanol (5×). Yields obtained were in the range of 60–80%. Typical ^1H NMR data (CDCl$_3$) δ: 7.48–6.22 (C_6H_5), 4.49–3.93 (C_5H_5, C_5H_4), 2.40–0.41(CH$_2$), 0.23 (s, CH$_3$). Detailed synthesis, complete characterization and electrochemical studies will be published elsewhere [31,32].

2.3. Apparatus

Electrochemical measurements were performed using an Ecochemie BV Autolab PGSTAT 12. The experiments were carried out in a conventional three-electrode cell at 20–21 °C with a Pt disk of 3 mm diameter as working electrode, a Pt wire as auxiliary electrode, and a BAS non-aqueous Ag/Ag$^+$ reference electrode or a saturated Calomel reference electrode (SCE) were employed in organic solvents or in aqueous media respectively. In steady-state measurements, an Autolab rotating-disk electrode was used and

the amperometric measurements were performed in 0.1 M phosphate buffer with 0.1 M NaClO$_4$ deoxygenated by bubbling high-purity nitrogen. The background current was allowed to decay to a steady value before aliquots of stock NADH or glucose solution were added.

[1]H nuclear magnetic resonance (NMR) spectra were recorded at a frequency of 300 MHz using a Bruker AC 300 or on a Bruker AMX 400 working at 400 MHz using deuterated chloroform as solvent.

Size exclusion chromatography (SEC) was performed on an instrument consisting of a Waters 717 plus autosampler, a TSP Spectra Series P 100 pump and a set of three PSS-SDV 5 μm columns with 100, 1000, and 10 000 Å porosity. THF was used as an eluent at 30 °C and at a flow rate of 1 mL min^{-1}. UV absorptions were studied by a SpectraSYSTEM UV2000. The specific refractive index increment (dn/dc) was measured at 30 °C on an Optilab DSP interferometric refractometer (also RI detector) and determined with the WYATT ASTRA IV software (Version 4.90.08).

2.4. Electrode preparation

The Pt disk electrode was polished using 0.1 μm alumina powder and rinsed with water in an ultrasonic bath. The electrode surface was then conditioned by cycling the potential between the limits for hydrogen and oxygen evolution in 0.5 M H$_2$SO$_4$ solution until well-defined cyclic voltammograms were obtained, and then rinsed with water.

Films of the corresponding ferrocenyl-functionalized polymers (**1**, **2** and **3**) were deposited on the above prepared surface from the electrolyte bath containing 1 mM in the redox active species (ferrocene) and 0.1 M tetrabutylammonium hexafluorophosphate in dichloromethane, which was deaerated with nitrogen prior to electrooxidation, under potentiostatic control at a potential of +0.8 V (vs. Ag/Ag$^+$ reference electrode). The coated electrodes were rinsed with dichloromethane.

The surface coverage of electroactive ferrocenyl sites in the films, Γ, was determined from the integrated charge of the cyclic voltammetric waves.

The polymer-modified electrodes were stored in ultrapure water at room temperature when not in use. The immobilization of the enzyme was carried out by immersing the polymer coated electrode in an electrochemical cell containing an enzyme solution (0.1% of GOx in acetate buffer, pH 5.3, and NaClO$_4$ 0.1 M). A +0.7 V vs. SCE potential was applied to the polymer coated electrodes during 30 min under stirring and nitrogen bubbling, subsequently the electrodes had been kept for 10 min in glutaraldehyde vapour at room temperature. The pH of the enzyme solution was kept at a value of 5.3 where the enzyme exists in the form of an anion, GOx^{m-}, facilitating its interaction with the oxidized copolymer. The prepared enzyme electrode was allowed to dry in air, and rinsed thoroughly with the buffer. The enzyme electrodes were stored in ultrapure water at 4 °C when not in use.

3. Results

3.1. Synthesis of ferrocenyl-functionalized block-copolymers

Three different block-copolymers with different fractions of styrene and butadiene units (10:1, 4:1 and 2:1) were prepared by anionic polymerization and subsequently functionalized at the PB-block with diferrocenylmethylsilane via hydrosilylation reaction. All block-copolymers **1a**–**3a** prepared and the respective ferrocene-functionalized materials **1**–**3** are listed in Table 1. For the hydrosilylation step, Karstedt's catalyst was employed, resulting in the organometallic block-copolymers PS$_m$–PB$_{n-p}$ (HSiMeFc$_2$)$_p$ where $m = 615$, $n = 53$, $p = 39$ (**1**), $m = 375$, $n = 92$, $p = 76$ (**2**) and

Table 1
SEC/MALLS/viscosimetry data of ferrocenyl-functionalized block-copolymers

Compound		Molar mass, M_n^a($\times 10^{-3}$ gmol^{-1})	PDI[a]	Viscometric radius, R_η^b (nm)
1a	PS$_{615}$–PB$_{53}$	66.9	1.02	6.2
1	PS$_{615}$–PB$_{53}$ (HSiMeFc$_2$)$_{39}$	98.6	1.04	6.6
2a	PS$_{375}$–PB$_{92}$	44.1	1.07	5.1
2	PS$_{375}$–PB$_{92}$ (HSiMeFc$_2$)$_{76}$	97.4	1.11	5.5
3a	PS$_{455}$–PB$_{204}$	58.4	1.02	5.7
3	PS$_{455}$–PB$_{204}$ (HSiMeFc$_2$)$_{170}$	157.0	1.10	6.5

[a] Determined via coupled SEC/MALLS.
[b] Molecular weight calculated from SEC with online viscosimetry.

$m = 455$, $n = 204$, $p = 170$ (**3**) (Scheme 1). Detailed structural analysis of the block-copolymers was achieved by a combination of SEC with multi-angle light-scattering detector and NMR-spectroscopy [32]. SEC chromatograms measured in THF demonstrate a small shift of the peak maximum to lower elution volumes, as expected. According to SEC, all block-copolymers exhibited narrow polydispersity index (PDI) in the range of 1.02–1.11 after ferrocene functionalization of the PB-block (Table 1), which translates to very well-defined polymer structures.

^{1}H NMR spectra of the ferrocenyl-containing copolymers combine the signals typical for the PS block (between 6.3 and 7.3 ppm the aromatic protons and between 0.8 and 2.4 ppm the backbone protons are observed [32]), with the pattern of resonances in the cyclopentadienyl region characteristic of the newly introduced monosubstituted ferrocenes (between 4.00 and 4.40 ppm) and the methylsilyl singlet at 0.23 ppm. Firm evidence for the diferrocenylsilane functionalization was provided by the almost complete disappearance of the olefinic protons of the PB-block at 5.45 and 4.94 ppm. Based on the signals intensities the ferrocene fractions were estimated to be in the range of 10 to nearly 50 wt % of ferrocene. This corresponds to a degree of functionalization of 73–83%.

3.2. Electrochemical behaviour of the copolymers

Cyclic voltammograms of the block-copolymers at low concentrations ($\sim 10^{-4}$ M in ferrocene centers) in CH$_2$Cl$_2$ solutions exhibit two well-separated and reversible oxidation systems of equal intensity (Fig. 1).

This two-wave redox response is similar to that observed for oligo- and poly(ferrocenylsilanes) reported by Manners and co-workers [2] and polysiloxanes functionalized with diferrocenylmethylvinylsilanes [33]. This electrochemical behaviour is consistent with the existence of appreciable interactions between the two iron centers bridged by a silicon atom. The initial oxidation occurs at non-adjacent ferrocene sites, which makes the subsequent removal of electrons from the remaining ferrocenyl centers, adjacent to those already oxidized more difficult.

In Fig. 1 it can be observed that the ΔE_p values of the cyclovoltammograms of the polymers obtained at a glassy carbon electrodes increase with increasing scan rates.

The corresponding standard rate constants for heterogeneous electron transfer (k^0) of the first electron step are given in Table 2, as estimated by the Nicholson's method [34], using the diffusion coefficients obtained from dynamic light scattering (DLS) [30]. It was also possible to determine the k^0 values for **1** and **2** by the application of the method of Milkin and Bard [35], employing rotating-disk electrode. The k^0 values determined in this way were 1.29×10^{-2} cm s^{-1} and 0.62×10^{-2} cm s^{-1} for **1** and **2**, respectively. All values obtained are comparable to standard rate constants for other reported macromolecules containing ferrocene groups [36].
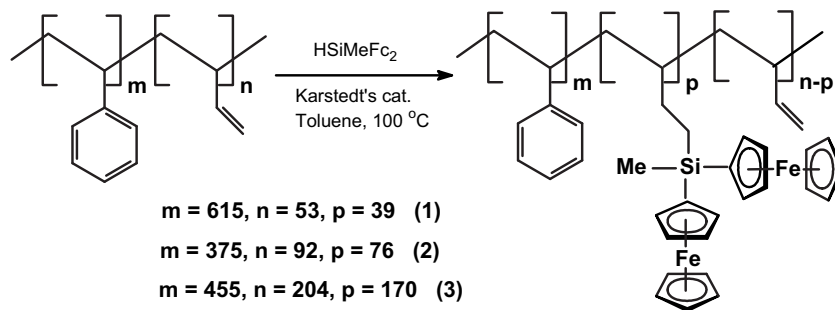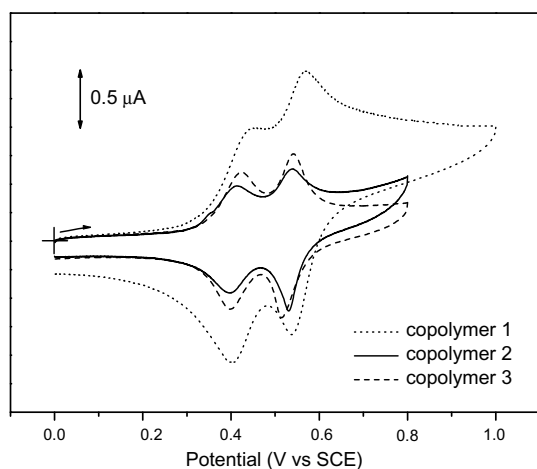
Scheme 1.

Fig. 1. Cyclic voltammograms of block-copolymers **1**, **2** and **3** solutions (10^{-4} M approx. in ferrocene centers) in CH_2Cl_2 with n-Bu$_4$NClO$_4$ 0.1 M as supporting electrolyte, measured at a Pt electrode with 100 mV s^{-1} scan rate.

Table 2
Electrochemical parameters for the block-copolymers

Compound	$^1E_{1/2}$ (V vs. SCE)[a]	$^2E_{1/2}$ (V vs. SCE)[a]	D_0 ($\times 10^6$ cm^2 s^{-1})[b]	k^0 (cm s^{-1})
1	0.43	0.55	0.61	1.7×10^{-2}
2	0.40	0.53	0.52	7.4×10^{-3}
3	0.41	0.52	0.55	3.0×10^{-3}

[a] Measured in CH_2Cl_2 with 0.1 M TBAP.
[b] Diffusion coefficients measured by D.L.S.

The architecture of the macromolecular structure to which the ferrocene substituents are attached seems to be essential for the accessibility in terms of electron transfer. The k^0 values reveal that the kinetics of electron transfer slows down with an increase of both the butadiene content and the block length ratio (PB/PS). This behaviour is related to the formation the coiled conformation of the block-copolymers. The experimental data suggest that the redox units are more shielded by the polymer chain, when the block-copolymer contains larger PB-diferrocenylsilane blocks. This finding is consistent with the ratios of experimental and theoretical peak currents observed in the cyclic voltammograms of copolymers previously reported [30].

3.3. Electrochemical behaviour of the modified electrodes

The block-copolymers were deposited onto electrode surfaces either by controlled potential electrolysis at +0.8 V (vs. SCE) or by performing a certain number of consecutive cycles between 0 and +1.2 V potential limits. Therefore the amount of electroactive material deposited can be controlled with the electrolysis time or the number of scans.

The microstructures of films of copolymers **2** and **3**, which contain lower amounts of styrene, electrochemically deposited on a platinum wire electrode (0.25 mm diameter) were examined by scanning electron microscopy. The SEM micrograph in Fig. 2A shows that the film of polymer **3** appears to be a relatively dense,
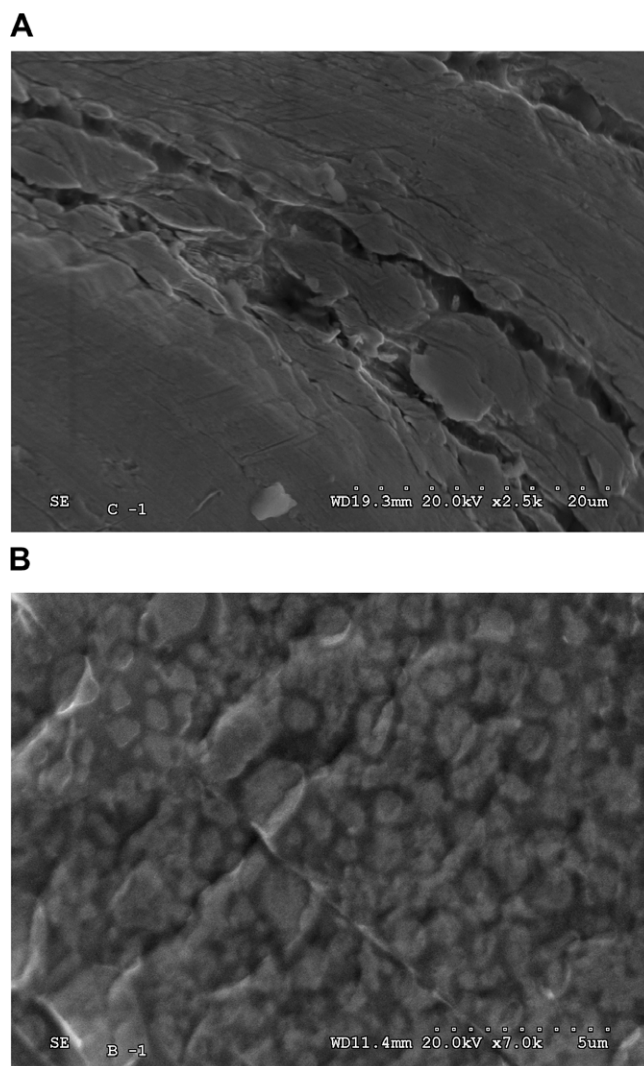

Fig. 2. SEM micrographs of the surface of platinum wire electrodes modified with films of copolymer **3** (A) and copolymer **2** (B).

multilayered material with a compact structure. The film formed by electrodeposition of copolymer **2** displays a less compact morphology consisting of randomly packed polymer aggregates (Fig. 2B). It is well known that this kind of polymers tend to phase separate in the bulk, if both blocks are immiscible, giving rise to cylindrical or lamellar domains. However, the influence of this nano-phase segregation was not the focus of our current work.

In non-aqueous (CH_2Cl_2) solutions, films of the three polymers deposited on platinum give a similar electrochemical response, which is reminiscent of the corresponding compounds in solution. The electrochemical properties of the modified electrodes are highly sensitive to the nature of the solution. As can be seen, in phosphate buffer solution the cyclic voltammograms display the peaks corresponding to the oxidation of the interacting ferrocenyl units practically overlapped with E_{pa} values of about 0.45 V (Fig. 3). The inclusion of polarizable solvent molecules between the ferrocene moieties and the formation of ion pairs with specific electrolyte anions probably counteract the electrochemical interaction and cause the merging of the two redox couples. A similar change in the features of the voltammetric responses caused by the action of polar solvents has been found in the case of poly(dialkylsilylene-ferrocenylene) films [37].

As indicated by Fig. 4 the anodic wave of the copolymers films appears at more positive potentials in the first scan than in succeeding scans. This is a break-in effect caused by the hydrophobic properties of the polymers which are initially poorly swollen by solvent and electrolyte. This break-in effect is also observed when modified electrodes are reused after storage in water.

The CV of an electrode modified with polymer **3** differs from the behaviour displayed by electrodes modified with **1** and **2**. In fact, in this case a much sharper signal is observed. This narrow wave can be attributed to attractive interactions between the electroactive centers within the film. This might be an indication of a special type of order on the electrode leading to a better stabilization of the oxidized polymer [38]. On other hand the features of the cyclovoltammograms of the three polymer-modified electrodes change, when they are stored in distilled water. As can be seen after several days the oxidation wave becomes broader, the I_{pa} values decrease slightly and ΔE_p values increase before a steady-state response is attained.

3.4. Catalytic oxidation of NADH at the modified electrodes

Fig. 5 shows the cyclic voltammograms for 2 mM NADH in aqueous phosphate buffer and a block-copolymer **3** modified plat-
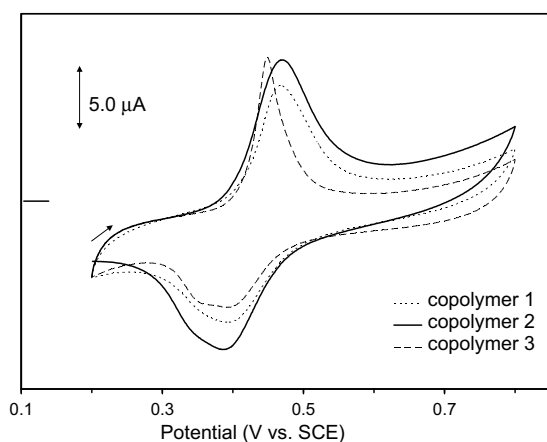

Fig. 4. Cyclic voltammograms of a Pt electrode modified with copolymer **3** ($\Gamma = 9.71 \times 10^{-10}$ mol ferrocene cm^{-2} thickness film) in 0.1 M deaerated phosphate buffer (pH 7.0), (A) second scan of a freshly prepared, (B) and (C) first and second scans respectively, of the same electrode stored in water at room temperature after two months. Scan rate 100 mV s^{-1}.

inum electrode. A catalytic wave is observed near 0.64 V hence the modified electrode decreases the overpotential required to oxidize NADH by 200 mV. A similar behaviour is displayed by electrodes modified with **1** and **2**.

This catalytic effect is explained by the diffusion of NADH to the electrode where it reduces the oxidized mediator to form NAD$^+$ and the reduced form of the mediator. This reaction is followed by the electrochemical reoxidation of the mediator:

$$NADH + M_{OX} \xrightarrow{k_1} M_{RED} + NAD^+ + H^+ \tag{1}$$

$$M_{RED} - 2e^- \rightarrow M_{OX} \tag{2}$$

$$\text{net}: \quad NADH \rightarrow NAD^+ + H^+ + 2e^- \tag{3}$$

The rate-determining step is given in Eq. (1) with a second-order rate constant k_1. Thus the reaction in Eq. (2) can be considered fast compared to that in Eq. (1).

The rate of the chemical reaction between NADH and the surface immobilized mediator (k_1, in M^{-1} s^{-1}) can be evaluated by cyclic voltammetry [39,40].

Fig. 3. Cyclic voltammograms of copolymers **1**, **2** and **3** deposited at platinum electrodes ($\Gamma \cong 9 \times 10^{-10}$ mol ferrocene cm^{-2} thickness film) in 0.1 M deaerated phosphate buffer (pH 7.0). Scan rate 100 mV s^{-1}.
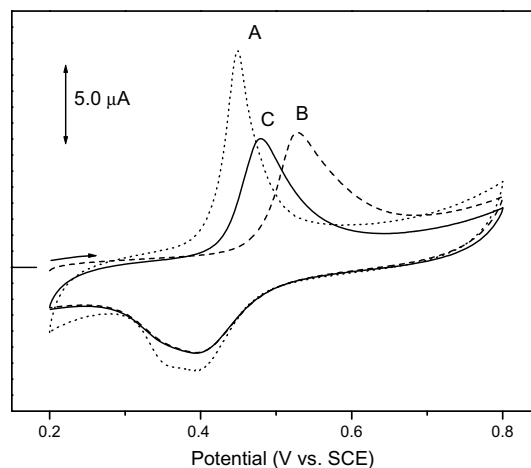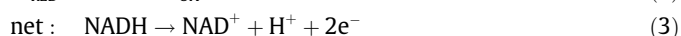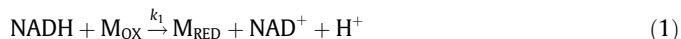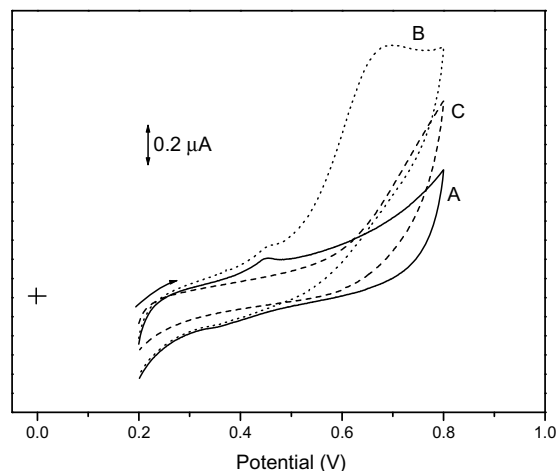

Fig. 5. Cyclic voltammograms of a copolymer **3** ($\Gamma = 1.0 \times 10^{-10}$ mol ferrocene cm^{-2} thickness film) coated platinum electrode in 0.1 M deaerated phosphate buffer (pH 7.0) solution in absence (A) and presence (B) of NADH 0.5 mM. (C) A platinum bare electrode in presence of NADH 0.5 mM. Scan rate 5 mV s^{-1}.

For the simplest case, in which only the mass transport of NADH and/or the rate constant k_1 can limit the reaction, E_p is [41]:

$$E_p = E^{0'} + \frac{RT}{nF}\left[0.78 + \ln\left(\frac{D_{NADH}^{1/2}}{k_1 \Gamma}\right) + \ln\left(\frac{nFv}{RT}\right)^{1/2} \right] \quad (4)$$

the currents of NADH oxidation were increased with the increase of the scan rate and the relationship between current and scan rate is as follows [42]:

$$i_p = 2.99 \times 10^5 n(\alpha n_a)^{1/2} AC_0 D_0^{1/2} v^{1/2} \quad (5)$$

where i_p, n, α, n_a, A, Γ, C_0, D_0, v are the peak current in ampere, the number of electrons transferred, the transfer coefficient, the apparent number of electrons involved in the rate-determining step, the electrode area in cm^2, the surface coverage, the bulk concentration in mol/cm^3, the diffusion coefficient in cm^2/s and the scan rate in V/s, respectively. In all cases the currents of NADH oxidation measured with electrodes modified with the three copolymers, increased with the increase of the scan rate, and the $i_p - v^{1/2}$ plots show linearity and demonstrate that the electrocatalytic oxidation is diffusion controlled.

The well known relationship between oxidation potential E_p and the peak current i_p is

$$i_p = 0.277 n FA C_0 k^0 e^{\left[\left(\frac{\alpha n_a F}{RT}\right)(E_p - E^{0'})\right]} \quad (6)$$

where $E^{0'}$ is the formal potential and k^0 the exchange heterogeneous rate constant in cm s^{-1} [43,44].

The values αn_a, n, and k^1 (obtained as $k^0 \Gamma^{-1}$) can easily determined from Eqs. (5) and (6). αn_a and k^0 are estimated respectively from the slope and the intercept of the graphs Ln i_p vs. E_p. The number of electrons, n, is provided by Eq. (5) once the αn_a values are known.

On other hand we have applied the model developed by Andrieux and Saveant [39] who derived a relation between the peak current and the concentration for the case when k_1 is infinitely fast:

$$i_p = 0.496 n FA D_0^{1/2} v^{1/2} C_0 \left(\frac{nF}{RT}\right)^{1/2} \quad (7)$$

They found that low values of k_1 result in lower values of the constant (0.496) and k_1 can be obtained from the plot provided by these authors of the "constant" variations vs. the logarithm of the "kinetic parameter":

$$\log \left[\frac{k_1 \Gamma}{D_0^{1/2}\left(\frac{nFv}{RT}\right)^{1/2}} \right] \quad (8)$$

Table 3 summarizes the electrochemical parameters obtained by both procedures for oxidation of NADH solutions at various pH. These rate constants are close to those previously reported for electrodes modified with other mediators such as 1,2-benzophenoxazine-7-one $(8 \times 10^2 \, M^{-1} \, s^{-1})$, 5-methylphenazinium $(1.5 \times 10^3 \, M^{-1} \, s^{-1})$, 4-methylcatechol $(3.3 \times 10^3 \, M^{-1} \, s^{-1})$ and poly(thionine) $(2.1 \times 10^3 \, M^{-1} \, s^{-1})$.

As can be observed in Table 3 the k_1 values show a slight increase as the pH of solutions increases. This fact can be explained,

since in the present case the mediator is a two-electron non-proton acceptor type and therefore the proton must be transferred to the contacting solution supporting material.

In general the k_1 values found for the electrocatalytic oxidation of NADH by the electrodes modified with the three different block-copolymers increase in the order polymer **1** < polymer **2** < polymer **3**, that parallels with the presence in the compound of larger ferrocenyl blocks. This behaviour can be attributed to the higher concentration of organometallic centers in **2** and **3**, which allows a more efficient charge transport in their films. Furthermore, this effect seems to prevail over other morphologic and structural effects because the interaction enzyme-electroactive sites should be easier into polymer **2** film than that expected for polymer **3**, according to the less compact morphology and more permeable structure of the electrodeposited layers of **2**.

On the other hand, it can be observed from Fig. 5 that the catalytic wave is not coincident with that of the mediator oxidation itself. As described previously [45] this can be due to the formation of a charge-transfer complex and the catalytic peak actually represents oxidation of the complex. The catalytic reaction process can be represented as

$$NADH + M_{OX} \leftrightarrow [NADH-M_{OX}] \rightarrow NAD^+ + H^+ + M_{RED} \quad (9)$$
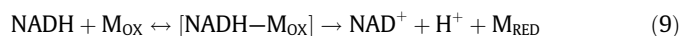
The oxidized mediator and NADH combine to form the charge-transfer complex, then the complex decomposes and NADH is oxidized to NAD$^+$ and M_{RED} is reoxidized at positive potentials.

This mechanism is confirmed by rotating-disk experiments. In the present case, the catalytic process was studied with an electrode modified with a copolymer **1** film (Fig. 6).[1] The rotating-disk electrode was kept at 0.85 V, within the potential range of the plateau obtained in the voltammetric curve at a low scan rate. Levich plots (i vs. $\omega^{1/2}$) reveal kinetic restrictions and the rate constants k_1 can be evaluated from the intercept of Koutecky–Levich plots (i^{-1} vs. $\omega^{-1/2}$) and are found to be $2.7 \times 10^3 \, M^{-1} \, s^{-1}$, $2.9 \times 10^3 \, M^{-1} \, s^{-1}$ and $3.0 \times 10^3 \, M^{-1} \, s^{-1}$ for NADH concentration 2, 3, and 4 mM respectively. At all instances the calculated value of the number of electrons is close to 2. As can be seen the values of k_1 are dependent of [NADH]. This fact has been observed for other mediator modified electrodes [43] and has been explained because the formation of a charge-transfer complex takes place in the catalytic oxidation of NADH.

Fig. 7 shows the dependence of anodic current for a copolymer **1** platinum modified electrode on NADH concentration at 500 mV applied potential. The sensor shows a sensitivity of 0.68 μA/mM and a detection limit of 16 μM ($S/N = 3$). It is seen that no linear dependence of the anodic current on coenzyme concentration is obtained. This behaviour is in agreement with a two-step electrocatalytic process that may be assumed to proceed, including the formation of a transient complex between NADH and the mediator [46,47].

3.5. Catalytic oxidation of glucose oxidase at the modified electrodes

The electrocatalytic application of these copolymers as mediators of glucose oxidase in the glucose oxidation has been also investigated. First of all the behaviour of the copolymers modified electrodes has been studied with GOx in solution. Fig. 8 shows the cyclic voltammogram of a copolymer **1** modified electrode in phosphate buffer at pH 7 containing 5 mg GOx. As it can be seen, in the presence of glucose a striking change in the cyclic voltammogram

Table 3
Kinetic parameters for NADH electrooxidation

Compound	n^a	$k_1 \times 10^{-3} \, M^{-1} \, s^{-1a}$			$k_1 \times 10^{-3} \, M^{-1} \, s^{-1b}$		
		pH 6.3	pH 7.0	pH 7.7	pH 6.3	pH 7.0	pH 7.7
1	2.3	1.8	2.2	2.6	1.7	2.8	2.7
2	2.2	3.5	3.5	3.6	2.7	3.7	3.9
3	1.8	3.8	4.0	7.2	6.1	4.5	9.8

[a] Obtained from cyclic voltammetry by Eqs. (5) and (6).
[b] Determined using the Andrieux–Saveant's relation.

---

[1] Data with poor reproducibility were obtained with copolymers **2** and **3**. Electrodes modified with these copolymers showed a great sensitivity to the application of high rotational speeds, probably due to the increase of the ionic concentration into the films, which affects the films conductivity.
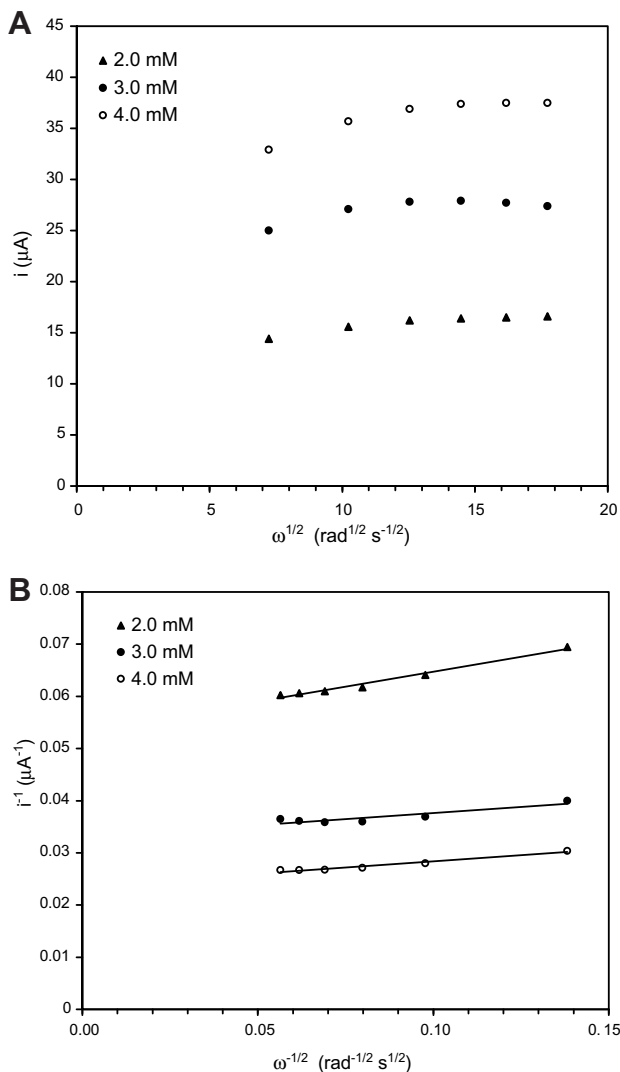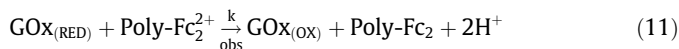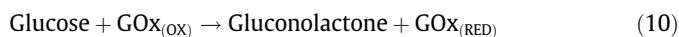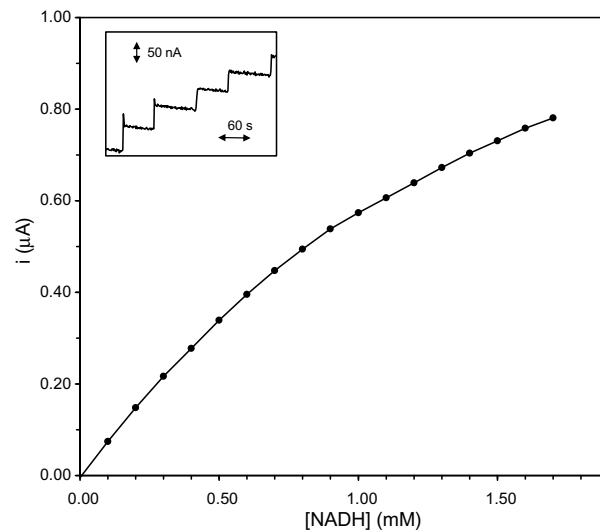
Fig. 7. Calibration curve for NADH oxidation at copolymer **1** modified platinum electrode ($\Gamma = 9.7 \times 10^{-10}$ mol ferrocene cm^{-2} thickness film) in 0.1 M deaerated phosphate buffer (pH 7.0). $E = 0.5$ V vs. SCE. Inset: typical current responses of the modified electrode to consecutive addition of 0.1 mM NADH aliquots. Each value is the mean result of five electrodes.
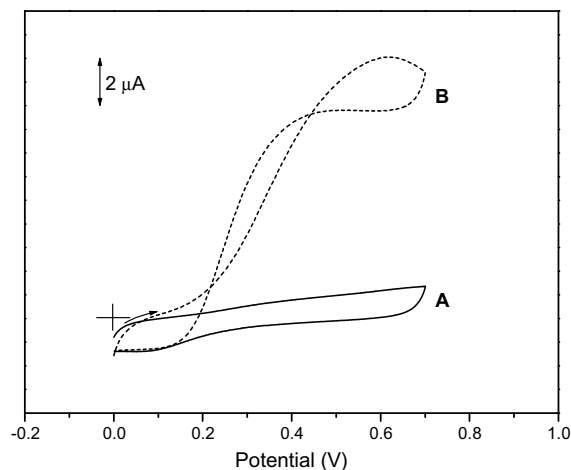

Fig. 6. (A) Levich and (B) Koutecky–Levich plots for the steady electrocatalytic response for a copolymer **1** modified platinum electrode ($\Gamma = 2.59 \times 10^{-10}$ mol ferrocene cm^{-2} thickness film) at different NADH concentrations in 0.1 M deaerated phosphate buffer (pH 7.7).

Fig. 8. Cyclic voltammograms of a copolymer **1** ($\Gamma = 9.69 \times 10^{-10}$ mol ferrocene cm^{-2} thickness film) coated platinum electrode in deaerated 10 mM glucose solution in 0.1 M phosphate buffer (pH 7.0) solution in absence (A) and presence (B) of 5 mg GOx. Scan rate 5 mV s^{-1}.

is observed and a remarkable enhancement of the oxidation peak is observed.

The reaction steps required to oxidize glucose and produce electrical current may be written as follows:

$$\text{Glucose} + \text{GOx}_{(OX)} \rightarrow \text{Gluconolactone} + \text{GOx}_{(RED)} \qquad (10)$$

$$\text{GOx}_{(RED)} + \text{Poly-Fc}_2^{2+} \xrightarrow{k_{obs}} \text{GOx}_{(OX)} + \text{Poly-Fc}_2 + 2\text{H}^+ \qquad (11)$$

$$\text{Poly-Fc}_2 \leftrightarrow \text{Poly-Fc}_2^{2+} + 2e^- \qquad (12)$$

The rate constant k_{obs} for reaction (11) can be derived from cyclic voltammetry measurements provided that the electron transfer from the reduced mediator to the electrode (12) is fast compared with the rate of the reaction between ferricinium ion and glucose oxidase, which takes place at the surface films, and there is a sufficient excess of substrate to ensure that the enzyme is fully reduced and the concentration of GOx$_{(red)}$ will effectively remain unchanged throughout the experiment.

The observed constant (k_{obs}) values determined from Eqs. (5) and (6) for electrodes modified with the copolymers **1–3** in glucose 50 mM, GOx 1.3×10^{-5} M, phosphate buffer pH 7.0 solution were

4.7×10^2 M^{-1} s^{-1}, 6.6×10^2 M^{-1} s^{-1} and 4.9×10^2 M^{-1} s^{-1} for the electrodes modified with **1**, **2** and **3** respectively.

The experimentally derived ratio of anodic current in the presence of enzyme (i_k) to the peak current in its absence (i_d) at a given scan rate may be taken as a measure of the catalytic efficiency of the modified electrodes [39]. For scan rate of 10 mV s^{-1} and films of the block-copolymers (surface coverage $\Gamma \cong 3.5 \times 10^{-10}$ mol cm^{-2}) the i_k/i_d values for **1**, **2** and **3** are 2.3, 2.7 and 3.0 respectively.

3.6. Glucose sensor properties

As a representative example the block-copolymer **2** has been evaluated as constituent of amperometric biosensors for D-Glucose. Glucose oxidase was immobilized into conducting films of the polymer by electrostatic interactions, employing the procedure described in Section 2.
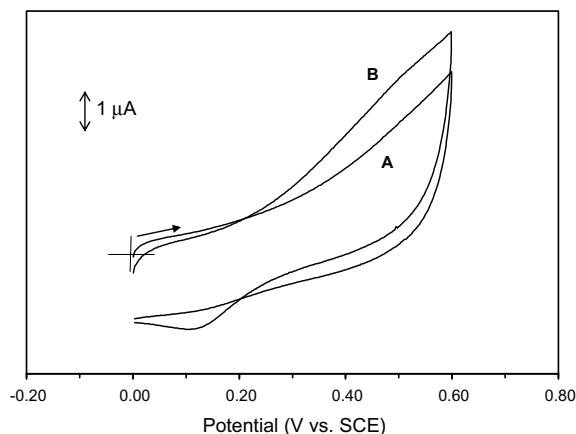
Fig. 9. Cyclic voltammograms of a platinum disk electrode modified with a film of copolymer **2** – GOx ($\Gamma = 8.8 \times 10^{-10}$ mol ferrocene per cm^{-2} thickness film) in 0.1 M deaerated phosphate buffer (pH 7.0) in absence (A) and presence (B) of glucose 5 mM. Scan rate 5 mV s^{-1}.

Fig. 10. Glucose calibration plot of copolymer **2** – enzyme sensor ($\Gamma = 8.8 \times 10^{-10}$ mol ferrocene cm^{-2} thickness films). Steady-state currents measured at + 0.30 V (vs. SCE), in 0.1 M deaerated phosphate buffer (pH 7.0). Each value is the mean result of five electrodes. Inset: typical current responses of the sensor to consecutive addition of 1 mM glucose aliquots.

In all cases, the optimal operational conditions in the immobilization process were employed. Immersion periods longer than 30 min or/and GOx concentrations higher than 0.1% did not give rise to variations in the results. Fig. 9 shows cyclic voltammograms of a polymer-GOx modified electrode taken in phosphate buffer (pH 7) before (curve A) and after (curve B) 5 mM of glucose were added to the solution. It should be appreciated that the redox peaks in Fig. 9A are not as prominent and intense as those of a polymer-modified electrode (without GOx immobilization, Fig. 3). The change in the shape of the cyclic voltammogram is usually observed and has been attributed to the effects of the GOx molecules (GOx^{m-}), incorporated by electrostatic interactions in the film structure, on the charge-transfer process. A similar electrochemical behaviour due to the counteranion effects has been previously reported for electrodes modified with films of polymers containing ferrocene units [16,48,49]. As can be observed in Fig. 9 the electrochemical behaviour of the enzyme electrodes is influenced by the presence of glucose in solution. When glucose was dissolved in the electrolyte solution, a remarkable increase in the oxidation current was observed at potentials more positive than 0.25 V vs. SCE, indicating that ferrocene molecules immobilized in the film are efficient electron mediators between the electrode substrate and the redox centers of FAD/GOx. In the presence of glucose the anodic wave increases, which is indicative of an enzyme-catalyzed process. In order to test the analytical performance of the enzyme electrodes calibration curves were obtained. Fig. 10 shows the steady-state currents for an electrode modified with copolymer 2 obtained at 0.3 V as a function of the glucose concentration for electrolyte solutions saturated with N$_2$. The biosensor responds quickly to the substrate additions with a good linear response region even at 300 mV (vs. SCE) working potential. A detection limit of 0.2 mM ($S/N = 3$) and a sensitivity of 50 nA/mM were obtained.

In agreement with the model developed by Savinell and co-workers [49], a non-linear Lineweaver–Burke plot (i^{-1} vs. substrate^{-1}) is qualitatively indicative of a mass transport limitation, and that the operating potential suffices to eliminate the electrolysis rate from consideration, this behaviour corresponds to a sensor in which the substrate diffusion becomes slower than other reaction steps [50].

In this kind of sensors, the slope of the calibration curves has a different significance that in the case of processes controlled by the rate of catalysis, because it is independent of the Michaelis–Menten constant [51] but dependent upon the diffusion coefficient of the substrate. If the film thickness is increased, the slope of the calibration plot decreases.
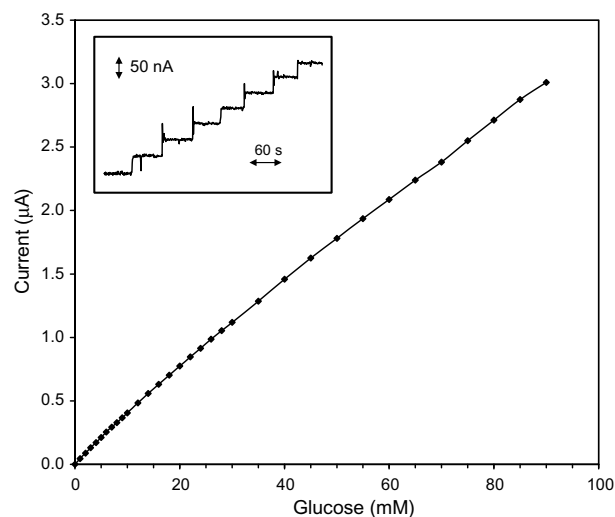
When the rate of the enzymatic reaction is mass transport controlled, a value for Michaelis–Menten constant may be calculated from the slope of the Lineweaver–Burke plot by extrapolation [51] but in fact it is an "effective" or "apparent" constant $K_{M,app}$, due to the diffusion limited process. The $K_{M,app}$ determined from L–B plots at an operating potential of 0.30 V was 72.7. This value of $K_{M,app}$ obtained is larger than the intrinsic value and the linearly measurable range is greatly enhanced. In fact, it has been reported previously that the linear range of glucose sensors can be increased substantially by using an additional polymer coating on the surface of the sensor [52,53]. In the same way, the copolymer probably provides an intrinsic resistance to the diffusion of glucose, due to the compact structure of the films.

The equivalent Michaelis constant obtained is lower than other reported constants for sensors based on similar ferrocene dendrimers and polymers [54,55]. This finding indicates that these block-copolymers with interacting ferrocenes are more efficient redox enzymatic mediators.

4. Conclusions

The electrochemical properties of a series of block-copolymers functionalized with interacting di(ferrocenyl)silanes have been examined. It has been found that the electrochemical behaviour of these polymers is affected by structural characteristics. As it was expected, the presence of polystyrene blocks confers long-term stability and reproducibility to the electrodes modified with block-copolymer films, which we attribute to the excellent film-forming properties of the polystyrene blocks. The results confirm that electrodes modified with the examined copolymers are efficient redox mediators for the electrocatalytic oxidation of both reduced nicotinamide dinucleotide cofactor and glucose oxidase. The reaction with NADH proceeds via formation of a charge-transfer intermediate before yielding the reaction products.

The rate constants are significantly higher than those previously found for electrodes modified with monomeric ferrocenes and comparable with the values reported for several different immobilized mediators. This is a novel example of electrodes modified with ferrocene derivatives that can be applied to the determination of NADH without the use of diaphorase.

The redox copolymers co-immobilized with glucose oxidase have also been successfully used as amperometric biosensors for glucose determinations. As expected these compounds allow using lower working potentials (0.25 V vs. SCE) that contributes to reduce the effect of the interfering electrochemical compounds. The sensitivities and detection limits obtained are comparable or even better than those of other ferrocene-modified polymer-mediator based electrodes. Further detailed work on the influence of the macromolecular architecture on the electrochemical properties of block- and random copolymers of the type introduced here is in progress.

Acknowledgements

References

[1] A. Togni, T. Hayashi (Eds.), Ferrocenes. Homogeneous Catalysis, Organic Synthesis, Materials Science, VCH, Weinheim, 1995.
[2] P. Nguyen, P. Lopez-Elipe, I. Manners, Chem. Rev. 99 (1999) 1515.
[3] G.R. Whittell, I. Manners, Adv. Mater. 19 (2007) 3439.
[4] I. Manners, in: I. Manners (Ed.), Synthetic Metal-Containing Polymers, Wiley-VCH, Weinheim, 2004, p. 237.
[5] P.A. Chase, R.J.M.K. Gebbink, G. van Koten, J. Organomet. Chem. 689 (2004) 4016.
[6] D. Astruc, in: A.S.A. Abd-El-Aziz, I. Manners (Eds.), Frontiers in Transition Metal-Containing Polymers, Wiley, Hoboken, NJ, 2007 (Chapter 11).
[7] S. Förster, T. Plantenberg, Angew. Chem. 41 (2002) 689.
[8] J. Rodríguez-Hernández, F. Chécot, Y. Gnanou, S. Lecommandoux, Prog. Polym. Sci. 30 (2005) 691.
[9] N. Hadjichristidis, S. Pispas, G. Floudas, Block Copolymers: Synthetic Strategies, Physical Properties, and Applications, Wiley-Interscience, NJ, 2003.
[10] D.G. Bucknall, H.L. Anderson, Science 302 (2003) 1904.
[11] O. Nuyken, V. Burkhardt, C. Hubsch, Macromol. Chem. Phys. 198 (1997) 3353.
[12] M. Baumert, J. Fröhlich, M. Stieger, H. Frey, R. Mülhaupt, H. Plenio, Macromol. Rapid Commun. 20 (1999) 203.
[13] D.A. Durkee, H.B. Eitouni, E.D. Gomez, M.W. Ellsworth, A.T. Bell, N.P. Balsara, Adv. Mater. 17 (2005) 2003.
[14] I. Manners, Angew. Chem. 46 (2007) 1565.
[15] B. Alonso, C.M. Casado, I. Cuadrado, M. Moran, A.E. Kaifer, Chem. Commun. (2002) 1778.
[16] M.P. García Armada, J. Losada, I. Cuadrado, B. Alonso, B. González, E. Ramírez-Oliva, C.M. Casado, Sensor. Actuat. B-Chem. 88 (2003) 190.
[17] M.P. García Armada, J. Losada, I. Cuadrado, B. Alonso, B. González, C.M. Casado, J. Zhang, Sensor. Actuat. B-Chem. 101 (2004) 143.
[18] F. Le Floch, H.A. Ho, P. Harding-Lepage, M. Bedard, R. Neagu-Plesu, M. Leclerc, Adv. Mater. 17 (2005) 1251.
[19] J.M. Gibbs, S.J. Park, D.R. Anderson, K.J. Watson, C.A. Mirkin, S.T. Nguyen, J. Am. Chem. Soc. 127 (2005) 1170.
[20] C. Ueda, DC-S. Tse, T. Kuwana, Anal. Chem. 54 (1982) 850.
[21] A. Torstensson, L. Gorton, J. Electroanal. Chem. 130 (1981) 199.
[22] B.W. Carlsson, LL. Miller, J. Am. Chem. Soc. 106 (1983) 3850.
[23] M.J. Lobo, A.J. Miranda, J.M. López-Fonseca, P. Tuñon, Anal. Chim. Acta 325 (1996) 33.
[24] D. Narasaiah, U. Spohn, L. Gorton, Enzyme Eng. XII 799 (1996) 482.
[25] L. Gorton, B. Persson, P.D. Hale, L.I. Boguslavsky, H.I. Karan, H.S. Lee, T.A. Skotheim, H.L. Lan, Y. Okamoto, in: P.G. Edelman, J. Wang (Eds.), Biosensors and Chemical Sensors, ACS Symposium Series, Am. Chem. Soc. 487 (1992) 56.
[26] M.V. Pishko, A.C. Michael, A. Heller, Anal. Chem. 63 (1991) 2268.
[27] N.C. Foulds, C.R. Lowe, Anal. Chem. 60 (1988) 2473.
[28] P.D. Hale, L.I. Boguslavsky, H. Inagaki, H.I. Karan, H.S. Lee, T.A. Skotheim, Y. Okamoto, Anal. Chem. 63 (1991) 677.
[29] J. Losada, M.P. Garcia Armada, I. Cuadrado, B. Alonso, B. Gonzalez, C.M. Casado, J. Zhang, J. Organomet. Chem. 689 (2004) 2799.
[30] A.G. Marcos, T.M. Pusel, R. Thomann, T. Pakula, L. Okrasa, S. Geppert, W. Gronski, H. Frey, Macromolecules 39 (2006) 971.
[31] F.J. López-Villanueva, A. García Marcos, K. Fischer, M. Schmidt, B. Alonso, C.M. Casado, M.P. García Armada, J. Losada, H. Frey, Am. Chem. Soc. 47 (2006) 1087.
[32] F.J. López-Villanueva, H. Schüle, A. García Marcos, B. de Juan, K. Fischer, M. Schmidt, B. Alonso, C.M. Casado, M.P. García Armada, J. Losada, H. Frey, in preparation.
[33] B. Alonso, B. González, B. García, E. Ramírez-Oliva, M. Zamora, C.M. Casado, I. Cuadrado, J. Organomet. Chem. 637 (2001) 642.
[34] R.S. Nicholson, Anal. Chem. 37 (1965) 1351.
[35] M.V. Milkin, A.J. Bard, Anal. Chem. 64 (1992) 2293.
[36] A.E. Kaifer, C.M. Cardona, J. Am. Chem. Soc. 120 (1998) 4023.
[37] H.T. Nguyen, A.F. Diaz, V. Dementev, K.H. Pannell, Chem. Mater. 6 (1994) 952.
[38] H.D. Abruña, Coord. Chem. Rev. 86 (1988) 135.
[39] C.P. Andrieux, J.M. Saveant, J. Electroanal. Chem. 93 (1978) 13.
[40] H. Jaegfeldt, T. Kuwana, G. Johansson, J. Am. Chem. Soc. 105 (1983) 1805.
[41] L. Gorton, J. Chem. Soc., Faraday Trans. 82 (1986) 1245.
[42] A.J. Bard, I.R. Faulkner, Electrochemical Methods, Wiley, New York, 1980.
[43] F.D. Munteanu, L.T. Kubota, L. Gorton, J. Electroanal. Chem. 509 (2001) 2.
[44] J. González Velasco, Electroanalysis 9 (1997) 880.
[45] Q. Chi, S. Dong, Analyst 119 (1994) 1063.
[46] A. Malinauskas, T. Ruzgas, L. Gorton, J. Colloid. Interf. Sci. 224 (2000) 35.
[47] M.J. Lobo, A.J. Miranda, P. Tuñon, Electroanalysis 9 (1997) 191.
[48] G. Inzelt, L. Szabo, Electrochim. Acta 31 (1986) 1381.
[49] Ch.J. Chen, Ch. Liu, R.F. Savinell, J. Electroanal. Chem. 348 (1993) 317.
[50] R.A. Kamin, G.S. Wilson, Anal. Chem. 52 (1980) 1198.
[51] L.D. Mell, J.T. Maloy, Anal. Chem. 47 (1975) 299.
[52] L. Boguslavsky, H. Kalash, Z. Xu, D. Beckles, L. Geng, T. Skotheim, V. Laurinavicius, H.S. Lee, Anal. Chim. Acta 311 (1995) 15.
[53] L. Gorton, H.I. Karan, P.D. Hale, T. Inagaki, Y. Okamoto, T.A. Skotheim, Anal. Chim. Acta 228 (1990) 23.
[54] B. Alonso, M.P. García Armada, J. Losada, I. Cuadrado, B. González, C.M. Casado, Biosens. Bioelectron. 19 (2004) 1617.
[55] J. Losada, M.P. García Armada, I. Cuadrado, B. Alonso, B. González, C.M. Casado, J. Zhang, J. Organomet. Chem. 689 (2004) 2799.